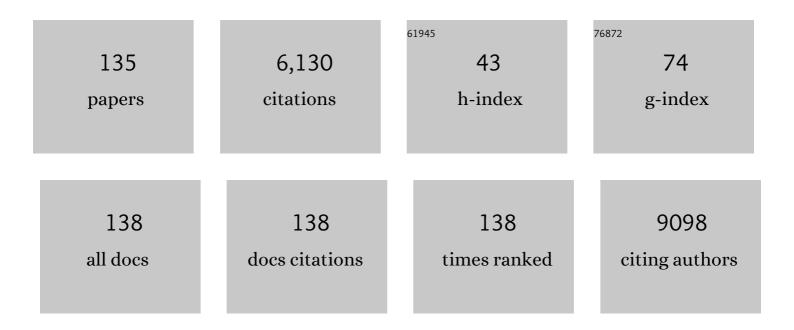
## List of Publications by Year in descending order

Source: https://exaly.com/author-pdf/9306410/publications.pdf Version: 2024-02-01



SEANILI

#	Article	IF	CITATIONS
1	Bifunctional water splitting enhancement by manipulating Mo-H bonding energy of transition Metal-Mo2C heterostructure catalysts. Chemical Engineering Journal, 2022, 431, 134126.	6.6	49
2	Nickel-Based Selenides with a Fractal Structure as an Excellent Bifunctional Electrocatalyst for Water Splitting. Nanomaterials, 2022, 12, 281.	1.9	27
3	Ultrahigh oxygen evolution reaction activity in Au doped co-based nanosheets. RSC Advances, 2022, 12, 6205-6213.	1.7	56
4	<i>In situ</i> phase transition induced TM–MoC/Mo <sub>2</sub> C (TM= Fe, Co, Ni, and Cu) heterostructure catalysts for efficient hydrogen evolution. Journal of Materials Chemistry A, 2022, 10, 10493-10502.	5.2	20
5	An atlas of room-temperature stability and vibrational anharmonicity of cubic perovskites. Materials Horizons, 2022, 9, 1896-1910.	6.4	8
6	Ferroelectric crystals with giant electro-optic property enabling ultracompact Q-switches. Science, 2022, 376, 371-377.	6.0	46
7	High-κ perovskite membranes as insulators for two-dimensional transistors. Nature, 2022, 605, 262-267.	13.7	109
8	Insight into the growth behaviors of MoS2 nanograins influenced by step edges and atomic structure of the substrate. Nano Research, 2022, 15, 7646-7654.	5.8	2
9	Accelerating CO2 reduction on novel double perovskite oxide with sulfur, carbon incorporation: Synergistic electronic and chemical engineering. Chemical Engineering Journal, 2022, 446, 137161.	6.6	34
10	Multitasking Memristor for High Performance and Ultralow Power Artificial Synaptic Device Application. ACS Applied Electronic Materials, 2022, 4, 3154-3165.	2.0	9
11	FeS2 bridging function to enhance charge transfer between MoS2 and g–C3N4 for efficient hydrogen evolution reaction. Chemical Engineering Journal, 2021, 421, 127804.	6.6	51
12	A comparative study of the structural and optical properties of Si-doped GaAs under different ion irradiation. Optical Materials, 2021, 111, 110611.	1.7	11
13	Defect engineering in perovskite oxide thin films. Chemical Communications, 2021, 57, 8402-8420.	2.2	22
14	Melamine Foam Derived 2H/1T MoS <sub>2</sub> as Flexible Interlayer with Efficient Polysulfides Trapping and Fast Li <sup>+</sup> Diffusion to Stabilize Li–S Batteries. ACS Applied Materials & Interfaces, 2021, 13, 6229-6240.	4.0	49
15	Strain-Directed Layer-By-Layer Epitaxy Toward van der Waals Homo- and Heterostructures. , 2021, 3, 442-453.		9
16	Superior Hydrogen Sorption Kinetics of Ti0.20Zr0.20Hf0.20Nb0.40 High-Entropy Alloy. Metals, 2021, 11, 470.	1.0	11
17	Vanadium doped 1T MoS2 nanosheets for highly efficient electrocatalytic hydrogen evolution in both acidic and alkaline solutions. Chemical Engineering Journal, 2021, 409, 128158.	6.6	98
18	Can Metal Intermixing Cooperatively Improve Perovskites as Redox Materials for Thermochemical Ammonia Synthesis? A Case Study on (Sr,Y)(Ti,Ru)O <sub>3</sub> . Journal of Physical Chemistry C, 2021, 125, 17019-17030.	1.5	2

#	Article	IF	CITATIONS
19	Tunable high acoustic impedance alumina epoxy composite matching for high frequency ultrasound transducer. Ultrasonics, 2021, 116, 106506.	2.1	13
20	Growth of High-Quality Monolayer Transition Metal Dichalcogenide Nanocrystals by Chemical Vapor Deposition and Their Photoluminescence and Electrocatalytic Properties. ACS Applied Materials & Interfaces, 2021, 13, 47962-47971.	4.0	14
21	New insights on the substantially reduced bandgap of bismuth layered perovskite oxide thin films. Journal of Materials Chemistry C, 2021, 9, 3161-3170.	2.7	9
22	Co–Al-substituted strontium hexaferrite for rare earth free permanent magnet and microwave absorber application. Journal Physics D: Applied Physics, 2021, 54, 024001.	1.3	42
23	Realization of exchange bias control with manipulation of interfacial frustration in magnetic complex oxide heterostructures. Physical Review B, 2021, 104, .	1.1	8
24	Electronic and nanostructure engineering of bifunctional MoS2 towards exceptional visible-light photocatalytic CO2 reduction and pollutant degradation. Journal of Hazardous Materials, 2020, 381, 120972.	6.5	90
25	Tuning catalytic performance by controlling reconstruction process in operando condition. Applied Catalysis B: Environmental, 2020, 260, 118103.	10.8	68
26	Binary Pd/amorphous-SrRuO3 hybrid film for high stability and fast activity recovery ethanol oxidation electrocatalysis. Nano Energy, 2020, 67, 104247.	8.2	55
27	Interface-Charge Induced Giant Electrocaloric Effect in Lead Free Ferroelectric Thin-Film Bilayers. Nano Letters, 2020, 20, 1262-1271.	4.5	95
28	Nitrogen/oxygen co-doped carbon nanofoam derived from bamboo fungi for high-performance supercapacitors. Journal of Power Sources, 2020, 479, 228835.	4.0	41
29	Effect of the geometry of precursor crucibles on the growth of MoS <sub>2</sub> flakes by chemical vapor deposition. New Journal of Chemistry, 2020, 44, 21076-21084.	1.4	1
30	Illumination-Induced Phase Segregation and Suppressed Solubility Limit in Br-Rich Mixed-Halide Inorganic Perovskites. ACS Applied Materials & Interfaces, 2020, 12, 38376-38385.	4.0	27
31	Single-Crystal-like Textured Growth of CoFe <sub>2</sub> O <sub>4</sub> Thin Film on an Amorphous Substrate: A Self-Bilayer Approach. ACS Applied Electronic Materials, 2020, 2, 3650-3657.	2.0	49
32	Manipulation of planar oxygen defect arrangements in multifunctional magnèli titanium oxide hybrid systems: from energy conversion to water treatment. Energy and Environmental Science, 2020, 13, 5080-5096.	15.6	15
33	Glassy Magnetic Transitions and Accurate Estimation of Magnetocaloric Effect in Ni–Mn Heusler Alloys. ACS Applied Materials & Interfaces, 2020, 12, 43646-43652.	4.0	3
34	Thermoelectric performance enhancement by manipulation of Sr/Ti doping in two sublayers of Ca3Co4O9. Journal of Advanced Ceramics, 2020, 9, 769-781.	8.9	24
35	A melt-diffusion strategy for tunable sulfur loading on CC@MoS2 for lithium–sulfurâ€< batteries. Energy Reports, 2020, 6, 172-180.	2.5	24
36	A review of Sb2Se3 photovoltaic absorber materials and thin-film solar cells. Solar Energy, 2020, 201, 227-246.	2.9	243

#	Article	IF	CITATIONS
37	One‧tep Synthesis of N/S Codoped "Porous Carbon Cloth―as a Sulfur Carrier for Lithium–Sulfur Batteries. Energy Technology, 2020, 8, 2000188.	1.8	11
38	Correlating the Composition-Dependent Structural and Electronic Dynamics of Inorganic Mixed Halide Perovskites. Chemistry of Materials, 2020, 32, 2470-2481.	3.2	20
39	Photocatalytic solar fuel production and environmental remediation through experimental and DFT based research on CdSe-QDs-coupled P-doped-g-C3N4 composites. Applied Catalysis B: Environmental, 2020, 270, 118867.	10.8	165
40	Promoting visible-light photocatalytic activities for carbon nitride based 0D/2D/2D hybrid system: Beyond the conventional 4-electron mechanism. Applied Catalysis B: Environmental, 2020, 270, 118870.	10.8	107
41	High-performance asymmetric supercapacitors realized by copper cobalt sulfide crumpled nanoflower and N, F co-doped hierarchical nanoporous carbon polyhedron. Journal of Power Sources, 2020, 456, 228023.	4.0	58
42	Steam-Assisted Chemical Vapor Deposition of Zeolitic Imidazolate Framework. , 2020, 2, 485-491.		26
43	Highly Conductive PDMS Composite Mechanically Enhanced with 3D-Graphene Network for High-Performance EMI Shielding Application. Nanomaterials, 2020, 10, 768.	1.9	16
44	Magnetic and Conductive Liquid Metal Gels. ACS Applied Materials & Interfaces, 2020, 12, 20119-20128.	4.0	73
45	The interplay among molecular structures, crystal symmetries and lattice energy landscapes revealed using unsupervised machine learning: a closer look at pyrrole azaphenacenes. CrystEngComm, 2019, 21, 6173-6185.	1.3	5
46	Multiple Anionic Transition-Metal Oxycarbide for Better Lithium Storage and Facilitated Multielectron Reactions. ACS Nano, 2019, 13, 11665-11675.	7.3	28
47	Au quantum dots engineered room temperature crystallization and magnetic anisotropy in CoFe <sub>2</sub> O <sub>4</sub> thin films. Nanoscale Horizons, 2019, 4, 434-444.	4.1	77
48	Superconductivity and structural instability in layered BiS <sub>2</sub> -based LaO <sub>1â^'x</sub> BiS <sub>2</sub> . Journal of Materials Chemistry C, 2019, 7, 586-591.	2.7	10
49	Structural Insight into Layer Gliding and Lattice Distortion in Layered Manganese Oxide Electrodes for Potassiumâ€ion Batteries. Advanced Energy Materials, 2019, 9, 1900568.	10.2	125
50	Manipulation of charge carrier concentration and phonon scattering via spin-entropy and size effects: Investigation of thermoelectric transport properties in La-doped Ca3Co4O9. Journal of Alloys and Compounds, 2019, 801, 60-69.	2.8	19
51	α-CsPbl <sub>3</sub> Colloidal Quantum Dots: Synthesis, Photodynamics, and Photovoltaic Applications. ACS Energy Letters, 2019, 4, 1308-1320.	8.8	65
52	One-step colloid fabrication of nickel phosphides nanoplate/nickel foam hybrid electrode for high-performance asymmetric supercapacitors. Chemical Engineering Journal, 2019, 373, 1132-1143.	6.6	120
53	Probing the Origin of Gold Dissolution and Tunneling Across Ni <sub>2</sub> P Shell Using in situ Transmission Electron Microscopy. ACS Applied Materials & Interfaces, 2019, 11, 46947-46952.	4.0	2
54	NH3-Sensing Mechanism Using Surface Acoustic Wave Sensor with AlO(OH) Film. Nanomaterials, 2019, 9, 1732.	1.9	14

#	Article	IF	CITATIONS
55	Recent Progress in Lithium Lanthanum Titanate Electrolyte towards All Solid-State Lithium Ion Secondary Battery. Critical Reviews in Solid State and Materials Sciences, 2019, 44, 265-282.	6.8	69
56	Improved densification and thermoelectric performance of In5SnSbO12 via Ga doping. Journal of Materials Science, 2018, 53, 6741-6751.	1.7	2
57	Functional Two-Dimensional Coordination Polymeric Layer as a Charge Barrier in Li–S Batteries. ACS Nano, 2018, 12, 836-843.	7.3	76
58	Sintering and electrical properties of commercial PZT powders modified through mechanochemical activation. Journal of Materials Science, 2018, 53, 13769-13778.	1.7	9
59	Recent Developments in Oxide-Based Ionic Conductors: Bulk Materials, Nanoionics, and Their Memory Applications. Critical Reviews in Solid State and Materials Sciences, 2018, 43, 47-82.	6.8	20
60	Digital to analog resistive switching transition induced by graphene buffer layer in strontium titanate based devices. Journal of Colloid and Interface Science, 2018, 512, 767-774.	5.0	43
61	Ultralight, highly flexible and conductive carbon foams for high performance electromagnetic shielding application. Journal of Materials Science: Materials in Electronics, 2018, 29, 13643-13652.	1.1	24
62	Thickness Dependence of Magnetic Behavior of LaAlO 3 /SrTiO 3 Heterostructures. Advanced Materials Interfaces, 2018, 5, 1800352.	1.9	6
63	Microscopic investigations of switching phenomenon in memristive systems: a mini review. RSC Advances, 2018, 8, 28763-28774.	1.7	9
64	Phase formation and microstructure evolution in mullite ceramics synthesized from mechanochemically activated oxide powders doped with Cr2O3. Journal of Physics and Chemistry of Solids, 2018, 123, 198-205.	1.9	5
65	Recent Advances of Layered Thermoelectric Materials. Advanced Sustainable Systems, 2018, 2, 1800046.	2.7	47
66	From Titanium Sesquioxide to Titanium Dioxide: Oxidation-Induced Structural, Phase, and Property Evolution. Chemistry of Materials, 2018, 30, 4383-4392.	3.2	42
67	The effects of composition deviations on the microstructure and thermoelectric performance of Ca3Co4O9 thin film. Journal of Materials Science: Materials in Electronics, 2018, 29, 13321-13327.	1.1	4
68	Synthesis of S-Doped porous g-C3N4 by using ionic liquids and subsequently coupled with Au-TiO2 for exceptional cocatalyst-free visible-light catalytic activities. Applied Catalysis B: Environmental, 2018, 237, 1082-1090.	10.8	151
69	Origins of possible synergistic effects in the interactions between metal atoms and MoS <sub>2</sub> /graphene heterostructures for battery applications. Physical Chemistry Chemical Physics, 2018, 20, 18671-18677.	1.3	7
70	Phosphorus-Based Alloy Materials for Advanced Potassium-Ion Battery Anode. Journal of the American Chemical Society, 2017, 139, 3316-3319.	6.6	755
71	Atomic Interface Engineering and Electricâ€Field Effect in Ultrathin Bi <sub>2</sub> MoO <sub>6</sub> Nanosheets for Superior Lithium Ion Storage. Advanced Materials, 2017, 29, 1700396.	11.1	343
72	A solution-processed TiS <sub>2</sub> /organic hybrid superlattice film towards flexible thermoelectric devices. Journal of Materials Chemistry A, 2017, 5, 564-570.	5.2	130

#	Article	IF	CITATIONS
73	Interfacial Redox Reactions Associated Ionic Transport in Oxide-Based Memories. ACS Applied Materials & Interfaces, 2017, 9, 1585-1592.	4.0	17
74	Defect induced charge trapping in C-doped α-Al2O3. Journal of Applied Physics, 2017, 122, 025702.	1.1	6
75	Tunable electronic and magnetic properties of arsenene nanoribbons. RSC Advances, 2017, 7, 51935-51943.	1.7	8
76	Magnetic Nanomaterials for Electromagnetic Wave Absorption. , 2017, , 473-514.		2
77	Manipulating resistive states in oxide based resistive memories through defective layers design. RSC Advances, 2017, 7, 56390-56394.	1.7	8
78	Subtle Interplay between Localized Magnetic Moments and Itinerant Electrons in LaAlO <sub>3</sub> /SrTiO <sub>3</sub> Heterostructures. ACS Applied Materials & Interfaces, 2016, 8, 13630-13636.	4.0	12
79	Electronic and Magnetic Properties of Transition-Metal-Doped Monolayer Black Phosphorus by Defect Engineering. Journal of Physical Chemistry C, 2016, 120, 9773-9779.	1.5	43
80	Oxygen Vacancy Dependence of Magnetic Behavior in the LaAlO 3 /SrTiO 3 Heterostructures. Advanced Materials Interfaces, 2016, 3, 1600547.	1.9	13
81	Novel synthesis and thermal property analysis of MgO–Nd2Zr2O7 composite. Ceramics International, 2016, 42, 16888-16896.	2.3	11
82	Enhanced Photovoltaic Effect in Feâ€Doped (Bi, Na) TiO <sub>3</sub> â€BaTiO <sub>3</sub> Ferroelectric Ceramics. International Journal of Applied Ceramic Technology, 2016, 13, 896-903.	1.1	9
83	UV irradiation induced reversible graphene band gap behaviors. Journal of Materials Chemistry C, 2016, 4, 8459-8465.	2.7	13
84	Phononic Structure Engineering: the Realization of Einstein Rattling in Calcium Cobaltate for the Suppression of Thermal Conductivity. Scientific Reports, 2016, 6, 30530.	1.6	1
85	Switching of magnetic easy-axis using crystal orientation for large perpendicular coercivity in CoFe2O4 thin film. Scientific Reports, 2016, 6, 30074.	1.6	148
86	Electronic and magnetic properties of Co doped MoS2 monolayer. Scientific Reports, 2016, 6, 24153.	1.6	94
87	Probing complementary memristive characteristics in oxide based memory device via non-conventional chronoamperometry approach. Applied Physics Letters, 2016, 108, 033506.	1.5	10
88	Large Piezoelectricity and Ferroelectricity in Mnâ€Doped (Bi <sub>0.5</sub> Na <sub>0.5</sub> )TiO <sub>3</sub> â€BaTiO <sub>3</sub> Thin Film Prepared by Pulsed Laser Deposition. Journal of the American Ceramic Society, 2016, 99, 2347-2353.	1.9	27
89	Tuning the surface oxygen concentration of {111} surrounded ceria nanocrystals for enhanced photocatalytic activities. Nanoscale, 2016, 8, 378-387.	2.8	163
90	A Facile and Template-Free One-Pot Synthesis of Mn3O4 Nanostructures as Electrochemical Supercapacitors. Nano-Micro Letters, 2016, 8, 165-173.	14.4	50

#	Article	IF	CITATIONS
91	Orbital engineering of two-dimensional materials with hydrogenation: A realization of giant gap and strongly correlated topological insulators. Physical Review B, 2015, 92, .	1.1	16
92	Evidence of Filamentary Switching in Oxide-based Memory Devices via Weak Programming and Retention Failure Analysis. Scientific Reports, 2015, 5, 13599.	1.6	37
93	Heterogeneous Distribution of Sodium for High Thermoelectric Performance of pâ€type Multiphase Leadâ€Chalcogenides. Advanced Energy Materials, 2015, 5, 1501047.	10.2	63
94	Ethanol-directed morphological evolution of hierarchical CeO <sub>x</sub> architectures as advanced electrochemical capacitors. Journal of Materials Chemistry A, 2015, 3, 13970-13977.	5.2	32
95	Periodicity Dependence of the Built-in Electric Field in (Ba <sub>0.7</sub> Ca <sub>0.3</sub> )TiO <sub>3</sub> /Ba(Zr <sub>0.2</sub> Ti <sub>0.8</sub> )O <sub>3Ferroelectric Superlattices. ACS Applied Materials &amp; Interfaces, 2015, 7, 26301-26306.</sub>	×4.0	23
96	Zn vacancy induced ferromagnetism in K doped ZnO. Journal of Materials Chemistry C, 2015, 3, 11953-11958.	2.7	43
97	Thermoelectric properties of sol–gel derived lanthanum titanate ceramics. RSC Advances, 2015, 5, 14735-14739.	1.7	11
98	The effect of annealing oxygen concentration in the transformation of Ca <sub>x</sub> CoO <sub>2</sub> to thermoelectric Ca <sub>3</sub> Co <sub>4</sub> O <sub>9</sub> . RSC Advances, 2015, 5, 28158-28162.	1.7	8
99	Dimensionality Controlled Octahedral Symmetry-Mismatch and Functionalities in Epitaxial LaCoO <sub>3</sub> /SrTiO <sub>3</sub> Heterostructures. Nano Letters, 2015, 15, 4677-4684.	4.5	71
100	Dehydrogenation: a simple route to modulate magnetism and spatial charge distribution of germanane. Journal of Materials Chemistry C, 2015, 3, 3128-3134.	2.7	7
101	Magnetic properties in α-MnO2 doped with alkaline elements. Scientific Reports, 2015, 5, 9094.	1.6	57
102	Strong Effect of Oxygen Partial Pressure on Electrical Properties of 0.5Ba(Zr <sub>0.2</sub> Ti <sub>0.8</sub> )O <sub>3</sub> –0.5(Ba <sub>0.7</sub> Ca <sub>0.3</sub> )TiO <su Thin Films. Journal of the American Ceramic Society, 2015, 98, 2094-2098.</su 	b <b>⊵.9</b> <td>&gt; 33</td>	> 33
103	The magnetism of <font>BiFeO</font> <sub>3</sub> powders. Functional Materials Letters, 2015, 08, 1550027.	0.7	0
104	Enhancement of the Stability of Fluorine Atoms on Defective Graphene and at Graphene/Fluorographene Interface. ACS Applied Materials & Interfaces, 2015, 7, 19659-19665.	4.0	39
105	Ferromagnetic ordering in Mn-doped ZnO nanoparticles. Nanoscale Research Letters, 2014, 9, 625.	3.1	61
106	Doping concentration dependence of microstructure and magnetic behaviours in Co-doped TiO2 nanorods. Nanoscale Research Letters, 2014, 9, 673.	3.1	32
107	XPS study of cobalt doped TiO <sub>2</sub> films prepared by pulsed laser deposition. Surface and Interface Analysis, 2014, 46, 1043-1046.	0.8	29
108	Voltage sweep modulated conductance quantization in oxide nanocomposites. Journal of Materials Chemistry C, 2014, 2, 10291-10297.	2.7	29

#	Article	IF	CITATIONS
109	Recent progress in high Bs and low Hc Fe-based nanocrystalline alloys. Nanotechnology Reviews, 2014, 3, .	2.6	8
110	Electric field manipulated reversible hydrogen storage in graphene studied by <scp>DFT</scp> calculations. Physica Status Solidi (A) Applications and Materials Science, 2014, 211, 351-356.	0.8	8
111	Tunable thermopower and thermal conductivity in Lu doped In2O3. RSC Advances, 2014, 4, 31926-31931.	1.7	9
112	Bipolar resistive switching characteristics in LaTiO3 nanosheets. RSC Advances, 2014, 4, 18127.	1.7	9
113	Improved super-capacitive performance of carbon foam supported CeO <sub>x</sub> nanoflowers by selective doping and UV irradiation. RSC Advances, 2014, 4, 35067-35071.	1.7	10
114	Thermoelectric properties of Yb and Nb codoped CaMnO <sub>3</sub> . Physica Status Solidi (A) Applications and Materials Science, 2014, 211, 1200-1206.	0.8	24
115	Improvement in the thermoelectric properties of CaMnO3 perovskites by W doping. Journal of Materials Science, 2014, 49, 7522-7528.	1.7	59
116	Evidencing the existence of intrinsic half-metallicity and ferromagnetism in zigzag gallium sulfide nanoribbons. Scientific Reports, 2014, 4, 5773.	1.6	8
117	Reversible Hydrophobic to Hydrophilic Transition in Graphene via Water Splitting Induced by UV Irradiation. Scientific Reports, 2014, 4, 6450.	1.6	105
118	Tuneable resistive switching characteristics of In2O3 nanorods array via Co doping. RSC Advances, 2013, 3, 13422.	1.7	23
119	Nickel foam based polypyrrole–Ag composite film: a new route toward stable electrodes for supercapacitors. New Journal of Chemistry, 2013, 37, 337-341.	1.4	59
120	Ga Substitution and Oxygen Diffusion Kinetics in Ca <sub>3</sub> Co <sub>4</sub> O <sub>9+δ</sub> -Based Thermoelectric Oxides. Journal of Physical Chemistry C, 2013, 117, 13382-13387.	1.5	32
121	Oxygen Migration in Dense Spark Plasma Sintered Aluminumâ€Doped Neodymium Silicate Apatite Electrolytes. Journal of the American Ceramic Society, 2013, 96, 3457-3462.	1.9	2
122	Crystallographic Orientation Dependence on Electrical Properties of ( <scp><scp>Bi</scp></scp> , <scp>Na</scp> ) <scp>TiO</scp> 3â€based Thin Films. Journal of the American Ceramic Society, 2013, 96, 3530-3535.	1.9	18
123	Stochastic memristive nature in Co-doped CeO2 nanorod arrays. Applied Physics Letters, 2013, 103, .	1.5	26
124	Zinc oxide nanotubes decorated with silver nanoparticles as an ultrasensitive substrate for surface-enhanced Raman scattering. Mikrochimica Acta, 2012, 179, 315-321.	2.5	25
125	K0.25Mn2O4nanofiber microclusters as high power cathode materials for rechargeable lithium batteries. RSC Advances, 2012, 2, 1643-1649.	1.7	44
126	Immobilization of Na Ions for Substantial Power Factor Enhancement: Site-Specific Defect Engineering in Na <sub>0.8</sub> CoO <sub>2</sub> . Journal of Physical Chemistry C, 2012, 116, 4324-4329.	1.5	12

#	Article	lF	CITATIONS
127	Giant stability of substituent Co chains in ZnO:Co dilute magnetic oxides. AIP Advances, 2012, 2, 042155.	0.6	1
128	Ab initio study of phase stability in doped TiO2. Computational Mechanics, 2012, 50, 185-194.	2.2	78
129	Power Factor Enhancement for Few-Layered Graphene Films by Molecular Attachments. Journal of Physical Chemistry C, 2011, 115, 1780-1785.	1.5	38
130	Sb <sub>2</sub> Te <sub>3</sub> Nanoparticles with Enhanced Seebeck Coefficient and Low Thermal Conductivity. Chemistry of Materials, 2010, 22, 3086-3092.	3.2	83
131	Enhanced Field Electron Emission Properties of Hybrid Carbon Nanotubes Synthesized by RFâ€PECVD. Chemical Vapor Deposition, 2009, 15, 291-295.	1.4	3
132	Size Dependence and Spatial Variation of Electronic Structure in Nonpolar ZnO Nanobelts. Journal of Physical Chemistry C, 2009, 113, 4804-4808.	1.5	7
133	Highly porous reticular tin–cobalt oxide composite thin film anodes for lithium ion batteries. Journal of Materials Chemistry, 2009, 19, 8360.	6.7	88
134	Atomic Stacking Configurations in Atomic Layer Deposited TiN Films. Journal of Physical Chemistry B, 2002, 106, 12797-12800.	1.2	4
135	Microtexture Mapping of Elecrtron Backscattered Diffraction in (Bi,Pb)2Sr2Ca2Cu3O10 Superconductor Tapes. Materials Research Society Symposia Proceedings, 2000, 659, 1.	0.1	0